Two-photon fluorescence imaging of live neurons using a multimode optical fiber

Raphaël Turcotte[1,2], Carla C. Schmidt[1], Martin J. Booth[2]*, and Nigel J. Emptage[1]*.

1. Department of Pharmacology, University of Oxford, Mansfield Road, Oxford OX1 3QT, United Kingdom

2. Department of Engineering Science, University of Oxford, Parks Road, Oxford OX1 3PJ, United Kingdom

***Corresponding authors**: nigel.emptage@pharm.ox.ac.uk and martin.booth@eng.ox.ac.uk

Abstract

An ability to optically visualize neurons and their subcellular components across brain regions is integral to our understanding of neuronal function[1]. Multimode optical fibers (MMFs), combined with wavefront control methods, have achieved minimally-invasive *in vivo* imaging of neurons in deep-brain regions with diffraction-limited spatial resolution[2-5]. To date MMF systems have been based on linear fluorescence and are therefore only able to perform two-dimensional imaging due to an absence of confocal filtering[6]. Here we report a method to achieve optical sectioning in live brain tissue by taking advantage of the nonlinearity of two-photon excited fluorescence (TPEF). In addition, we provide a new approach for the determination of transmission matrix for TPEF, a necessary step for the light shaping requirement of MMF imaging. Central to these advances is the use of a laser source able to generate both continuous wave (CW) light and femtosecond pulses. This configuration allows the system to be compact with minimal distal optics, enhancing suitability for neuroscience applications. With our system we demonstrate TPEF imaging of neurons and their dendrites in live brain slices through a single 60 μm-core MMF with a numerical aperture of 0.37. Taken together these developments represent an important step towards three-dimensional (3D) deep-brain imaging *in vivo*.

28 **Main text**

29 Step-index MMFs have emerged as a central component of a minimally-invasive micro-endoscope
30 technology owing to their small size relative to other devices[2]. Indeed, their diameter, between 60-
31 150 µm, enables direct insertion several centimeters into the living mammalian brain while causing
32 minimal tissue damage and, hence, is likely to be of minimal consequence to the neuronal network[2-
33 5]. An essential component of MMF technology is wavefront control, required to circumvent the
34 random phase delays and mode coupling that occurs inside a fiber[7,8]. By shaping the wavefront
35 entering a MMF using a spatial light modulator (SLM), a diffraction-limited focused point of light
36 can be formed at the distal end of the fiber, suitable for the excitation of fluorophores in a sample.
37 Digital point-scanning can be realized by updating the SLM pattern and thus translating the focal
38 volume. Although the axial location of the focal plane can be precisely controlled, imaging is not 3D
39 when illuminating with one-photon excitation; out-of-focus background excitation is present,
40 restricting the use of the technology to sparsely labelled samples[2]. Confocality has been demonstrated
41 using reflectance contrast using a digital pinhole[6], however, the broad emission spectra of
42 fluorophores mean it is challenging to translate this approach to fluorescence imaging. The
43 importance of multiphoton processes for intrinsic 3D imaging is well recognized and femtosecond
44 laser pulses have been spatiotemporally focused[9] through MMFs for TPEF[10] and coherent anti-Stokes
45 Raman scattering[11] imaging as well as for microfabrication[12]. Unfortunately, these optical systems
46 require substantial distal optics and have not been shown to be compatible with biological imaging.
47 We sought to address this limitation and have developed a MMF system capable of multiphoton
48 imaging in living tissue. The device is optimized for translation into neuroscience research, although
49 we anticipate that it will also be suitable for other biological applications.

50 The central concept for the work is the use of a dual mode laser source, able to switch between
51 CW and pulsed operation (Mira Optima 900-F, Coherent, 830 nm). The light source was integrated
52 in an optical system that has been optimized for live animal imaging through compactness[13], stability,
53 and mobility[2]. Indeed, the modular design of the system is particularly well suited for *in vivo*

54 applications (Fig. 1); a detailed description is provided in the Supplementary Methods. Light from
55 the source module was directed toward an imaging module using free-space optics and to a calibration
56 module using a single mode optical fiber (SMF). The fixed imaging module comprised a liquid-
57 crystal SLM (LC-SLM) for modulating the wavefront, a pinhole for filtering undesired diffraction,
58 and optics to relay and couple the light from the LC-SLM into the MMF[2,13-15]. The movable
59 calibration module was used in the evaluation of the transmission matrix, which describes the
60 complex field propagation through the MMF, by imaging a selected plane some distance away from
61 the MMF distal facet while it interfered with the SMF reference beam[16]. A transmission matrix,
62 evaluated with the laser in CW mode, was used to calculate the patterns required on the LC-SLM for
63 shaping the wavefront such that the foci for digital point-scanning could be generated in the biological
64 sample at the plane of calibration[3]. Importantly, this configuration enabled us to evaluate the
65 transmission matrix with minimal distal optics, eliminating the need to position a focused beam with
66 free-space optics at the distal end of the fiber, and also to easily remove the distal optics in order to
67 position the specimen for imaging. These changes afford a substantial improvement in the technology
68 for neuroscience and life science applications.

69 The performance of our system was first assessed by generating foci at the MMF distal end
70 for multiphoton fluorescence excitation. For this purpose, illumination foci were sequentially
71 captured using the calibration module for both laser operating modes (Fig. 2). With CW light, a near
72 diffraction-limited light distribution was achieved in the center of the fiber (full width at half
73 maximum (FWHM): 2.6 ± 0.1 μm; $1/e^2$ width: 4.3 ± 0.2 μm). A maximum intensity projection of
74 illumination foci recorded at different lateral locations revealed that the performance was maintained
75 across the field-of-view (Fig. 2a), that is, uniform illumination was achieved. With the calibration
76 performed in CW mode, it was then necessary to switch to pulsed mode to generate multiphoton
77 fluorescence. The change in the laser temporal mode had minimal impact on the illumination foci
78 despite the high sensitivity of the transmission matrix to perturbations (Fig. 2b)[17]. With the laser in
79 pulse mode the width of the illumination foci increased (FWHM: 2.9 ± 0.1 μm) and tapered off more

80 slowly at the edges than for the CW mode (Fig. 2e; $1/e^2$ width: 5.7 ± 0.6 μm). Some deterioration in
81 the focus quality was expected because calibration is wavelength dependent and spectral broadening
82 would occur on transitioning from CW to pulsed mode (Fig. 2d; FWHM CW: 1.9 ± 0.3 nm; FWHM
83 pulse: 9.8 ± 0.3 nm). However, it is important to recognize that as the intensity of TPEF is dependent
84 on the square of the photon distribution, then the square of the illumination foci (Fig. 2b) should be
85 evaluated to characterize the TPEF excitation profile (Fig. 2c). When assessed in this way, a similar
86 point quality is achieved in pulsed mode as for the CW mode, with a FWHM of 2.5 ± 0.1 μm with
87 almost entirely suppressed extended edges (Fig. 2e; $1/e^2$ width: 4.0 ± 0.1 μm). Thus, we have
88 successfully implemented spatial focusing of femtosecond laser pulses through the MMF.

89 Having established a procedure for generating the desired light distribution in the sample, we
90 tested the TPEF imaging capability of the MMF system using fluorescent beads. Figure 3a shows an
91 image of 2-μm red fluorescent beads acquired at a distance of 40 μm from the distal facet of a MMF
92 25 mm in length with a core diameter of 60 μm and a numerical aperture of 0.37. An excellent signal-
93 to-noise ratio was achieved (SNR = 6.0 ± 0.6) with a total incident power at the sample of ~10 mW.
94 The fluorescence background from the focal plane has been a limiting factor for attaining high
95 dynamic range imaging. While the enhancement in peak intensity at the focus can easily reach values
96 between 100 and 350 over the average background illumination[3,4], the background fluorescence from
97 bright objects in the focal plane but outside the desired focus can easily overwhelm the signal from a
98 dim object at the focus, especially considering that the fluorescence background from all pixels is
99 integrated. Further suppression of the in-focus background from the nonlinearity of TPEF would
100 therefore be beneficial for increasing the dynamic range of the imaging system (Supplementary Fig.
101 S1).

102 As our design is optimized for live-tissue imaging we assessed its performance by imaging
103 Alexa Fluor 594 labelled neurons in live brain slices from the rat hippocampus. Fluorescent structures
104 were readily located and could be identified as neuronal cell soma (Fig. 3b). Pyramidal cell apical
105 dendrites were also clearly visible projecting from the soma. In an attempt to visualize smaller

features, we followed an apical dendrite away from the cell body and were able to detect secondary dendritic branching from the primary apical dendrite (Fig. 3c and Supplementary Fig. S1). The ability to visualize healthy cells within living tissue represents an important step for multiphoton MMF applications as previous demonstrations have all been confined to artificial samples[10,11]. Two particular challenges are faced when imaging live-tissue imaging: the first, achieving an adequate signal from the living structure, and the second, minimising phototoxic damage. Our successful imaging illustrates that these issues can be surmounted. Beyond the 3D imaging capability of the multiphoton approach, the intrinsic optical sectioning of nonlinear optical processes also reduces the out-of-focus fluorescence background, previously a considerable impediment for routine *in vivo* MMF imaging with linear fluorescence.

In summary, we have achieved multiphoton imaging of neurons and their dendrites in living brain tissue using wavefront control through a MMF. This is the first demonstration of this type and was accomplished by integrating a dual CW/pulsed laser source into a micro-endoscopic system that enabled spatial focusing of femtosecond pulses with minimal distal optics. We expect that this method will enable 3D imaging of densely labelled mammalian brains *in vivo* once implemented at optimized wavelengths and not just 830 nm. In addition, with enhancement in speed and computation, it is anticipated that it will be possible to improve focusing by maximizing point-by-point the nonlinear fluorescent signal obtained with the current calibration procedure. Increased computing capacity will also support MMFs with higher numerical aperture, e.g. from 0.37 to 0.66, offering control over a larger number of fiber modes, and thus substantial increase signal generation and collection for TPEF. Finally, we observed that the non-linearity of the multiphoton process exacerbated non-uniformities in the illumination. However, these non-uniformities are independent of the calibration method as they arise intrinsically from the fiber geometry and could be alleviated by performing spatially-variant deconvolution in order to make more regular the spatial response[18].

Acknowledgements

RT, CCS, MJB and NE acknowledge support from the Biotechnology and Biological Sciences Research Council (BBSRC) (BB/P0273OX/1). RT and MJB acknowledge support from the European Research Council (ERC) (H2020, 695140).

Conflict of Interest

The authors declare no conflict of interest.

References

1. Ji, N. The practical and fundamental limits of optical imaging in mammalian brains. *Neuron* **83,** 1242–1245 (2014).
2. Vasquez-Lopez, S. A. *et al.* Subcellular spatial resolution achieved for deep-brain imaging in vivo using a minimally invasive multimode fiber. *Light Sci. Appl.* **7,** 110 (2018).
3. Turcotte, R., Schmidt, C. C., Emptage, N. J. & Booth, M. J. Focusing light in biological tissue through a multimode optical fiber: refractive index matching. *Opt. Lett.* **44,** 2386–2389 (2019).
4. Ohayon, S., Caravaca-Aguirre, A., Piestun, R. & DiCarlo, J. J. Minimally invasive multimode optical fiber microendoscope for deep brain fluorescence imaging. *Biomed. Opt. Express* **9,** 1492–1509 (2018).
5. Turtaev, S. *et al.* High-fidelity multimode fibre-based endoscopy for deep brain in vivo imaging. *Light Sci. Appl.* **7,** 92 (2018).
6. Loterie, D. *et al.* Digital confocal microscopy through a multimode fiber. *Opt. Express* **23,** 23845 (2015).
7. Dholakia, K. & Čižmár, T. Shaping the future of manipulation. *Nat. Photonics* **5,** 335–342 (2011).

8. Di Leonardo, R. & Bianchi, S. Hologram transmission through multi-mode optical fibers. *Opt. Express* **19,** 247–254 (2011).

9. Morales-Delgado, E. E., Farahi, S., Papadopoulos, I. N., Psaltis, D. & Moser, C. Delivery of focused short pulses through a multimode fiber. *Opt. Express* **23,** 9109–9120 (2015).

10. Morales-Delgado, E. E., Psaltis, D. & Moser, C. Two-photon imaging through a multimode fiber. *Opt. Express* **23,** 32158–32170 (2015).

11. Trägårdh, J. *et al.* Label-free CARS microscopy through a multimode fiber endoscope. *Opt. Express* **27,** 30055–30066 (2019).

12. Morales-Delgado, E. E. *et al.* Three-dimensional microfabrication through a multimode optical fiber. *Opt. Express* **25,** 7031 (2017).

13. Plöschner, M. & Čižmár, T. Compact multimode fiber beam-shaping system based on GPU accelerated digital holography. *Opt. Lett.* **40,** 197–200 (2015).

14. Neil, M. A., Booth, M. J. & Wilson, T. Dynamic wave-front generation for the characterization and testing of optical systems. *Opt. Lett.* **23,** 1849–1851 (1998).

15. Čižmár, T. & Dholakia, K. Shaping the light transmission through a multimode optical fibre: complex transformation analysis and applications in biophotonics. *Opt. Express* **19,** 18871–18884 (2011).

16. Popoff, S. M. *et al.* Measuring the transmission matrix in optics: an approach to the study and control of light propagation in disordered media. *Phys. Rev. Lett.* **104,** 100601 (2010).

17. Loterie, D., Psaltis, D. & Moser, C. Bend translation in multimode fiber imaging. *Opt. Express* **25,** 6263–6273 (2017).

18. Lauer, T. R. Deconvolution with a spatially-variant PSF. in *Astronomical Data Analysis II. Proc. of SPIE*, 167–173 (2002).

179 *Figure legends*

180 **Figure 1. A dual mode laser enables multiphoton imaging with a MMF system optimized for**
181 **minimally invasive deep-brain micro-endoscopy.** Schematic of the experimental system. (**a**) The
182 source module contains a laser able to generate CW and pulse outputs. (**b**) The imaging module
183 includes an SLM for wavefront control during imaging and calibration, as well as a PMT for detection
184 of the epi-propagating signal. (**c**) The calibration module is used for recording illumination focus data
185 from the imaging module and, with the reference beam from the source module, for evaluating the
186 transmission matrix. *CW*: continuous wave; *PBS*: polarizing beam splitter; *SMF*: single-mode fiber;
187 *SLM*: spatial light modulator; *DM*: dichroic mirror; *MMF*: multimode fiber; *PMT*: photomultiplier
188 tube; *OL*: objective lens; *NPBS*: non-polarizing beam splitter; *CCD*: charge-couple device camera.

189 **Figure 2. TPEF nonlinearity facilitates wavefront control for focusing light through a MMF.**
190 (**a,b**) Illumination foci achieved with wavefront control through a MMF and recorded sequentially at
191 different positions (maximum intensity projection) when the laser is operating in (**a**) CW mode and
192 (**b)** pulsed mode. (**c**) Squared of the intensity distribution shown in (b) to illustrate the TPEF spots.
193 Scale bar: 15 µm; inset width: 7.6 µm. (**d**) Spectra of the laser source in CW and pulsed mode. (**e**)
194 Intensity profile for the inset foci shown in a-c.

195 **Figure 3. MMF multiphoton imaging of live brain tissue reveals neuronal bodies and dendrites.**
196 (**a**) Multiphoton image of red fluorescent beads (2 µm in diameter) acquired through a MMF. (**b**,**c**)
197 Multiphoton images in live brain tissue from the rat hippocampus acquired through a MMF showed
198 clearly identifiable (**b**) neuronal cell bodies and apical dendrites as well as (**c**) smaller dendrites
199 branching off from an apical dendrite, after the labelling of 2 to 3 neurons with AlexaFluor594. Scale
200 bar: 15 µm.

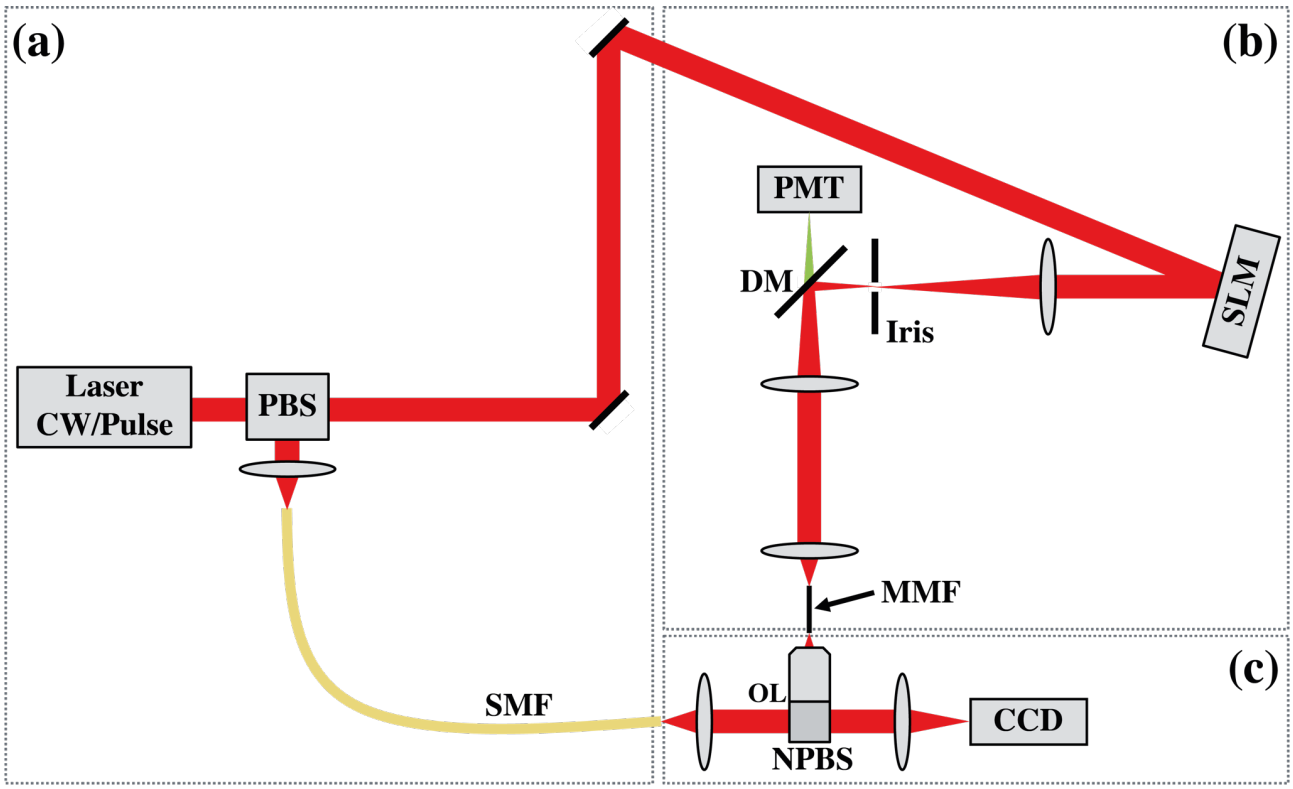

Figure 1

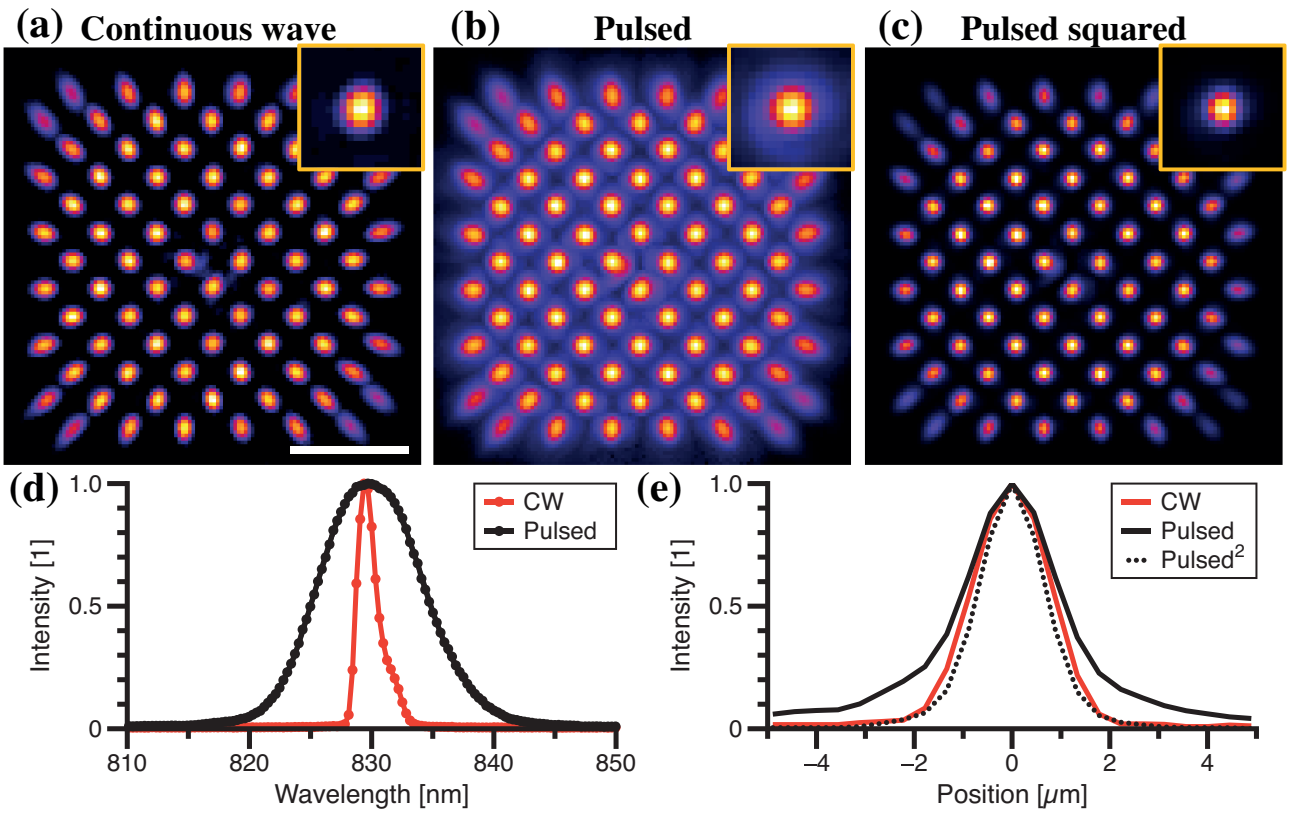
(a) Continuous wave
(b) Pulsed
(c) Pulsed squared
(d)
Intensity [1]
1.0
0.5
0
810
820
830
840
850
Wavelength [nm]
CW
Pulsed
(e)
Intensity [1]
1.0
0.5
0
–4
–2
0
2
4
Position [μm]
CW
Pulsed
Pulsed²

Figure 2

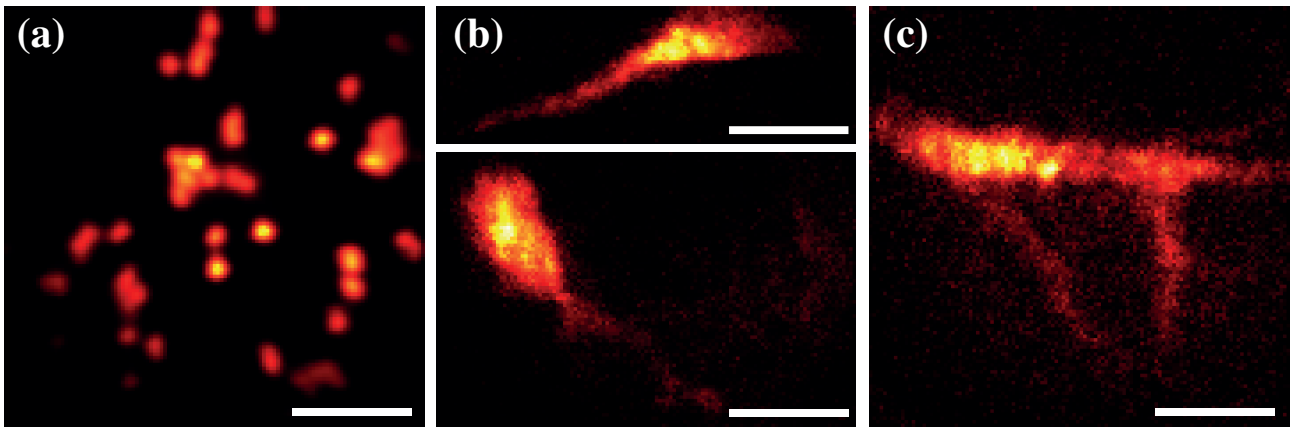

Figure 3